

Cite this: *RSC Adv.*, 2014, 4, 36834

Design and syntheses of novel fluorescent organosilicon-based chemosensors through click silylation: detection of biogenic amines†

Gurjaspreet Singh,^{*a} Satinderpal Singh Mangat,^a Hemant Sharma,^b Jandeep Singh,^a Aanchal Arora,^a Ajay Pal Singh Pannu^c and Narinder Singh^{*b}

A concise and useful synthesis of novel 1,2,3-triazole based silatrane (TBS)-scaffolds (**2a–e**) in good yield from 1,2,3-triazole based triethoxysilane (TBTES)-linkers (**1a–e**) is described. Click silylation of terminal alkynes with γ -azidopropyltriethoxysilane (AzPTES) was used for the synthesis of TBTES-linkers (**1a–e**). The synthesized TBS-scaffolds (**2a–e**) were comprehensively characterized by ^1H and ^{13}C NMR, mass spectrometry and single X-ray crystallographic studies. The broad scope of these TBS-scaffolds towards biogenic amines is explored by the use of a $\text{CH}_3\text{CN} : \text{H}_2\text{O}$ (98 : 2; v/v) solvent system. The receptor **2c** and **2d** shows high affinity towards spermine and histamine, respectively. To the best of our knowledge, the present investigation represents the first report on the use of organosilicon-based chemosensors for the recognition of biogenic amines.

Received 15th March 2014

Accepted 24th July 2014

DOI: 10.1039/c4ra02270j

www.rsc.org/advances

Introduction

The term “Click Silylation” encompasses the strategies of click and organosilicon chemistry that results into a powerful strategy for the synthesis of 1,2,3-triazole based triethoxysilane (TBTES)-linkers, which are known for their immense biological and medicinal properties.^{1–3} This research arena has received considerable attention owing to its aptitude to irreversibly couple two reactive molecular modules under ambient reaction conditions.^{4–11} In order to augment the scope of TBTES-linkers, it is planned to modulate the precursor molecule for the synthesis of fluorogenic organosilicon-based chemosensor (1,2,3-triazole-based silatrane TBS-scaffolds). This approach has several advantages such as: (a) it is a general method that can be readily extended to an extensive range of materials, including proteins, micelles, dye molecules and hybrid biomaterials;^{12–15} (b) unlike TBTES-linkers, assembled TBS-scaffolds are stable to hydrolyze, oxidize and reduce; (c) the ability of the N(3) atom of the 1,2,3-triazole and O(3) atom of the silatrane ring to act as a hydrogen bond acceptor even makes it more attractive in supramolecular chemistry.

In continuation to our research motivated by sensor development for analytes of environmental and biological importance,^{16–20} the present work is focused to develop sensors for biogenic amines, which are organic nitrogenous bases that regulate several physiological processes like body temperature, pH of the stomach, the immune response, brain activity, gastric acid secretion, cell growth and differentiation.^{21–27} These amines may have endogenous origins (low concentration) or be produced from microbial decarboxylation of amino acids (high concentration). A high content of these amines, especially spermine, spermidine, putrescine and histamine, causes intoxication in food; therefore, the level of these amines in food is used as an index of food quality.^{28,29} The estimation of spermine concentration in urine is an important parameter to check the presence of tumors and monitor the effectiveness of cancer therapy.³⁰ Various methods are available for the detection of biogenic amines like gas chromatography,³¹ thin-layer LC (liquid chromatography),^{32,33} reversed phase LC^{34–36} and LC with pre-column and post-column.^{37–39} Some of these techniques are extensively used due to low detection limits, high sensitivity and more accuracy,^{40,41} while a huge setup, long estimation times and the pretreatment of samples decreased the popularity of these methods. Chemosensors are better alternatives for the estimation of biogenic amines because they provide on-site detection, low detection limits and a broad detection range. However, only few chemosensors have been reported to date and most of them are based on polymers, nanoparticles, hydrogel and polyelectrolytes.^{42–45} We herein report an interesting application of click silylation with the aim to assemble TBS-scaffolds, which may offer a number of imperative advantages as chemosensors. The interesting

^aDepartment of Chemistry and Centre of Advanced in Chemistry, Panjab University, Chandigarh, 160014, India. E-mail: gjsingh@pu.ac.in; nsingh@iitrpr.ac.in

^bDepartment of Chemistry, Indian Institute of Technology, Ropar, 140001, Punjab, India

^cInstitute of Fundamental Sciences, Massey University, Private Bag 11 222, Palmerston North, New Zealand

† Electronic supplementary information (ESI) available. CCDC 982459 982458, 982460, 982461. For ESI and crystallographic data in CIF or other electronic format see DOI: 10.1039/c4ra02270j

Table 1 A comparison of analytical parameters of present method with literature reported

Method	Limit of detection	Sample pretreatment	Analysis time	Reproducibility
Enzyme based nanosensor ⁴⁶	1.1 mM for histamine	—	—	—
Enzyme sensor array ⁴⁷	10 mg kg ⁻¹ for histamine	Extraction and neutralization	3 min per sample	High, if using same electrode
HPLC ⁴⁸	0.5–2 mg kg ⁻¹ depending upon the amine	Extraction, neutralization, liquid–liquid extraction or solid phase extraction	30 min	Very high
Present methodology	7 μ M for spermine, 5 μ M for histamine	Filtration and centrifugation	2 min	High

feature of this methodology is the estimation of the spermine level in the urine samples. For diagnosis and treatment of tumors, estimation of spermine in urine is very helpful. Therefore, receptor **2c** was successfully utilized to detect the amount of spermine in urine samples from tumor patients. The comparison of analytical parameters for the general methods with the present technique is shown in Table 1.^{46–48} To the best of our knowledge, it is the first attempt to recognize biogenic amines through organosilicon chemistry.

Experimental section

Caution

Azide compounds are explosive to heat and shock. Great care and protection are needed when heating these compounds.

General material

All the syntheses were carried out under a dry nitrogen atmosphere using a vacuum glass line. The organic solvents used were dried and purified according to the standard procedure⁴⁹ and stored under dry nitrogen atmosphere. Bromotris(triphenylphosphine)copper(i) (Aldrich), 3-chloropropyltriethoxysilane (Aldrich), propargyl alcohol (Aldrich), phenyl acetylene (Aldrich), triethanolamine (Merck), tris(isopropyl)amine (ALDRICH), propargyl bromide (Aldrich), sodium azide (SDFCL), morpholine (Fischer Scientific), phthalimide (ALDRICH), potassium hydroxide (SDFCL) were used as supplied. IR spectroscopic data was recorded on a Thermo Scientific NICOLET iS50 FTIR instrument. ¹H and ¹³C NMR spectra were recorded on a Bruker Advance II 400 and JOEL 300 NMR spectrometer (in CDCl₃) at 25 °C. Chemical shifts were reported in ppm relative to internal CDCl₃ and external tetramethylsilane (TMS). Mass spectral measurements (ESI source with capillary voltage, 2500 V) were carried out on a VG Analytical (70-S) spectrometer. The compounds (3-azidopropyl)-triethoxysilane, *N*-(propargyl)-morpholine, *N*-(propargyl)-phthalimide, 2-(prop-2-yn-1-yloxy)benzaldehyde used as a starting material in the present study were prepared according to published procedures.^{1a} The absorption spectra were measured on a Specord 250 Plus Analytikjena spectrophotometer using quartz cells having a 1 cm path length. The fluorescence spectra were recorded on a Perkin Elmer L55 spectrofluorimeter with scanning speed 400, excitation and emission slit width was 10 nm. The pH of the solutions was recorded on a Toschon pH meter.

Recognition studies

All studies were performed in a CH₃CN–H₂O (98 : 2, v/v) solvent system. To get rid of kinetic errors, each spectrum was recorded after 15 min at 25 °C. The selectivity of ligands was evaluated by UV-Visible and emission spectroscopy. The biogenic amine assay was performed in 5 mL volumetric flasks having 10 μ M of ligand along with the particular amine (histamine, spermine, spermidine, tyramine, 1,2-diaminopropane, 1,4-diaminobutane, 1,5-diaminopentane, 2-phenylethylamine). For the selected amines, titrations were performed by the successive addition of the particular amine into a solution of the respective host (10 μ M). The binding constant was calculated by the Benesi–Hildebrand plot method, and the linear regression method was employed to determine the detection limit. The stoichiometry between amine and receptor was confirmed through Job's plot.⁵⁰ The maxima in the plot between [HG] and [H]/[H] + [G] corresponded to the stoichiometry of the complex.

X-ray structure determination

X-ray data of TBS-scaffolds **2a**, **2b**, **2d** and **2e** were recorded at low temperatures with a Rigaku-Spider X-ray diffractometer, comprising a Rigaku MM007 microfocus copper rotating-anode generator, high-flux Osmic monochromating and focusing multilayer mirror optics (Cu K radiation, λ = 1.5418 Å), and a curved image-plate detector. CrystalClear^{51a} was utilized for data collection and FSPProcess in PROCESS-AUTO^{51b} for cell refinement and data reduction. The structures were solved by direct methods using SIR97^{51c} and refined by full-matrix least-squares refinement techniques on F2 using SHELXL-97^{51d} in the WINGX package^{51e} of programs. Note that all non-hydrogen atoms were refined anisotropically. All other hydrogens were attached geometrically riding on their respective carrier atoms with Uiso being 1.5, 1.2, and 1.2 times the Uiso of their carrier methyl, methylene, and aromatic carbon atoms, respectively. The data measurement and other refinement parameters for these five crystal structures are given in Table 3.

Synthesis of compounds

Synthesis of 1-(3-(triethoxysilyl)propyl)-1H-(1,2,3-triazol-4-yl)-benzene (1a). A 50 mL two-necked, round-bottomed flask was filled with phenyl acetylene (0.50 g, 4.90 mmol), AzPTES (1.21 g, 4.90 mmol), triethylamine (3.0 mL), and tetrahydrofuran (3.0 mL) under nitrogen atmosphere in the presence of [CuBr(PPh₃)₃] (cat. amount), and the mixture was stirred at 60 °C

for 5 h. The reaction mixture was allowed to cool, and then the solvents were removed under reduced pressure, followed by the addition of hexane and then the mixture was filtered. The filtrate was concentrated under reduced pressure to afford the title compound as a brownish liquid in good yield. Yield: 1.40 g, 83%. IR (neat): 2963, 2928, 2876, 1664, 1459, 1370, 1185, 965, 762 cm^{-1} . ^1H NMR (300 MHz, CDCl_3): δ_{H} = 7.77–7.64 (m, 3H), 7.24 (m, 3H), 4.29 (t, J = 7.0 Hz, 2H), 3.72 (q, J = 7.0 Hz, 6H), 2.09–1.83 (m, 2H), 1.14 (t, J = 7.0 Hz, 9H), 0.66–0.44 (m, 2H). ^{13}C NMR (75 MHz, CDCl_3): δ_{C} = 130.6, 128.3, 127.5, 58.0, 53.3, 51.9, 23.9, 18.0, 7.2.

Synthesis of *N*-((1-(3-(triethoxysilyl)propyl)-1*H*-1,2,3-triazol-4-yl)-methyl)phthalimide (1b). This compound was synthesized following a similar procedure as for **1a**. However, *N*-(prop-2-ynyl)-phthalimide (2.0 g, 10.81 mmol), AzPTES (2.67 g, 10.81 mmol), and $[\text{CuBr}(\text{PPh}_3)_3]$ (cat. amount) were used here. Yield: 4.0 g, 85%. IR (neat): 2928, 2873, 1718, 1585, 1424, 1117, 908, 770 cm^{-1} . ^1H NMR (400 MHz, CDCl_3): δ_{H} = 7.77 (dd, J = 5.4, 3.1 Hz, 2H), 7.64 (dd, J = 5.5, 3.0 Hz, 2H), 7.54 (s, 1H), 4.91 (s, 2H), 4.24 (t, J = 7.2 Hz, 2H), 3.71 (q, J = 7.0 Hz, 6H), 1.95–1.88 (m, 2H), 1.12 (t, J = 7.0 Hz, 9H), 0.54–0.46 (m, 2H). ^{13}C NMR (100 MHz, CDCl_3): δ_{C} = 166.5, 132.9, 130.9, 122.3, 121.8, 57.40, 51.37, 32.02, 23.14, 17.24, 6.48.

Synthesis of 2-((1-(3-(triethoxysilyl)propyl)-1*H*-1,2,3-triazol-4-yl)-methoxy)benzaldehyde (1c). This compound was synthesized following a similar procedure as for **1a**. However, 2-(prop-2-ynyloxy)-benzaldehyde (1.0 g, 6.25 mmol), AzPTES (1.56 g, 6.31 mmol) and $[\text{CuBr}(\text{PPh}_3)_3]$ (cat. amount) were used here. Yield: 1.50 g, 92%. IR (neat): 2922, 2872, 1680, 1599, 1454, 1285, 1190, 1055, 911, 939, 775, 702, 655, 584 cm^{-1} . ^1H NMR (300 MHz, CDCl_3): δ_{H} = 10.36 (s, 1H), 7.71 (d, J = 7.0 Hz, 2H), 7.46 (s, 1H), 7.14–6.93 (m, 2H), 5.25 (s, 2H), 4.31 (t, J = 7.1 Hz, 2H), 3.72 (q, J = 8.6 Hz, 6H), 1.99–1.95 (m, 2H), 1.13 (t, J = 8.5 Hz, 9H), 0.52–0.47 (m, 2H). ^{13}C NMR (75 MHz, CDCl_3): δ_{C} = 188.8, 160.4, 135.6, 128.5, 125.7, 121.0, 112.5, 62.4, 58.2, 52.2, 23.9, 18.1, 7.2.

Synthesis of *N*-((1-(3-(triethoxysilyl)propyl)-1*H*-1,2,3-triazol-4-yl)methyl)morpholine (1d). This compound was synthesized following a similar procedure as for **1a**. However, *N*-(propargyl)-morpholine (1.10 g, 4.45 mmol), AzPTES (0.56 g, 4.45 mmol) and $[\text{CuBr}(\text{PPh}_3)_3]$ (cat. amount) were used here. Yield: 1.57 g, 95%. IR (neat): 2958, 2927, 1454, 1285, 1073 cm^{-1} . ^1H NMR (400 MHz, CDCl_3): δ_{H} = 7.43 (s, 1H), 4.28 (t, J = 7.2 Hz, 2H), 3.74 (q, J = 7.0 Hz, 6H), 3.65–3.61 (m, 4H), 3.59 (s, 2H), 2.47–2.41 (m, 4H), 1.99–1.91 (m, 2H), 1.15 (t, J = 7.0 Hz, 9H), 0.56–0.50 (m, 2H). ^{13}C NMR (100 MHz, CDCl_3): δ_{C} = 143.8, 132.08, 128.4, 122.5, 66.7, 58.47, 53.7, 53.4, 53.2, 24.1, 18.1, 7.4.

Synthesis of (1-(3-(triethoxysilyl)propyl)-1*H*-1,2,3-triazol-4-yl)-methanol (1e). This compound was synthesized following a similar procedure as for **1a**. However, propargyl alcohol (0.50 g, 8.92 mmol), AzPTES (2.20 g, 8.92 mmol) and $[\text{CuBr}(\text{PPh}_3)_3]$ (cat. amount) were used here. Yield: 2.50 g, 92%. IR (neat): 3364, 2930, 2875, 1460, 1309, 1271, 1080, 754 cm^{-1} . ^1H NMR (300 MHz, CDCl_3): δ_{H} = 7.46 (s, 1H), 4.71 (s, 2H), 4.65 (s, 1H), 4.23 (t, J = 6.9 Hz, 2H), 3.72 (q, J = 7.0 Hz, 6H), 1.98–1.88 (m, 2H), 1.14 (t, J = 7.0 Hz, 9H), 0.52–0.47 (m, 2H). ^{13}C NMR (75 MHz, CDCl_3): 147.7, 121.8, 58.1, 55.6, 52.1, 23.8, 17.9, 7.1.

1-(3-(Silatranyl)propyl)-1*H*-(1,2,3-triazol-4-yl)benzene (2a). Compound **1a** (1.0 g, 2.86 mmol) and a catalytic amount of potassium hydroxide was added to the stirred solution of triethanolamine (0.42 g, 2.86 mmol) in toluene (50.0 mL) in a 100.0 mL round-bottomed flask fitted with a Dean–Stark apparatus. The reaction mixture was then refluxed at 110 $^{\circ}\text{C}$ for 5 h. The reaction mixture was brought to room temperature slowly in 1 h. Toluene was removed under vacuum and on the slow addition of dry hexane (5.0 mL), a clear white solid precipitated out. The contents were further stirred for 1 h at room temperature. The solid was filtered and washed twice with dry diethylether (2 \times 5.0 mL) and dried under vacuum. The resulting solid was further dissolved in 20.0 mL of a 1 : 1 mixture of chloroform–ethanol and heated until a clear solution was obtained, which was then cooled slowly to room temperature and kept undisturbed for 5 days. White, thin shining needle-like crystals in star-shaped clusters suitable for single crystal X-ray analysis were isolated at room temperature. M.pt: 141 $^{\circ}\text{C}$. Yield: 0.80 g, 78%. IR (neat): 2960, 2931, 2876, 1665, 1459, 1370, 1344, 1185, 1050, 965, 762, 692, 540 cm^{-1} . ^1H NMR (300 MHz, CDCl_3): δ_{H} = 7.78–7.74 (m, 3H), 7.32–7.36 (m, 2H), 7.30 (s, 1H), 4.37 (t, J = 5.8 Hz, 2H), 3.77 (t, J = 5.8 Hz, 6H), 2.82 (t, J = 5.8 Hz, 6H), 2.00–2.06 (m, 2H), 0.61–0.36 (m, 2H). ^{13}C NMR (75 MHz, CDCl_3): δ_{C} = 128.7, 127.7, 125.6, 119.7, 55.6, 53.5, 50.9, 26.5, 13.3. MS (ES⁺) calcd for $\text{C}_{17}\text{H}_{25}\text{N}_4\text{O}_3\text{Si}$ $[\text{M} + \text{H}]^+$ 361.2, found 361.2; mass fragmentation (EI): 384 (13.7), 383 (65.5), 361 (100), 319 (11.9), 216 (3.9), 206 (7.7), 192 (8.4), 174 (27.7).

***N*-((1-(3-(Silatranyl)propyl)-1*H*-1,2,3-triazol-4-yl)methyl)phthalimide (2b).** This compound was synthesized following a similar procedure as for **2a**. However, triethanolamine (0.41 g, 2.78 mmol) and compound **1b** (1.20 g, 2.78 mmol) were used here. M.pt: 147 $^{\circ}\text{C}$, yield: 1.10 g, 89%, IR (neat): 2928, 2873, 1718, 1566, 1424, 1397, 1091, 908, 770, 712, 612, 578 cm^{-1} . ^1H NMR (400 MHz, CDCl_3): δ_{H} = 7.85 (dd, J = 5.4, 3.1 Hz, 2H), 7.71 (dd, J = 5.5, 3.0 Hz, 2H), 7.62 (s, 1H), 4.98 (s, 2H), 4.27 (t, J = 8.0 Hz, 2H), 3.75 (t, J = 5.8 Hz, 6H), 2.81 (t, J = 5.8 Hz, 6H), 1.99–1.91 (m, 2H), 0.51–0.26 (m, 2H). ^{13}C NMR (100 MHz, CDCl_3): δ_{C} = 167.7, 142.2, 134.0, 132.1, 128.3, 123.4, 122.7, 59.1, 57.5, 53.4, 51.0, 33.2, 13.2. MS (ES⁺) calcd for $\text{C}_{20}\text{H}_{26}\text{N}_5\text{O}_5\text{Si}$ $[\text{M} + \text{H}]^+$ 444.2, found 444.3; mass fragmentation (EI): 482 (100), 483 (19.7), 462 (18.5), 444 (7.6), 402 (6.8), 279 (5.2), 192 (4.5), 174 (10.2), 150 (17.2), 132 (11.5).

2-((1-(3-(Silatranyl)propyl)-1*H*-1,2,3-triazol-4-yl)methoxy)benzaldehyde (2c). This compound was synthesized following a similar procedure as for **2a**. However, Compound **1c** (1.0 g, 2.45 mmol) and triethanolamine (0.36 g, 2.45 mmol) were used here. M.pt: 137 $^{\circ}\text{C}$. Yield: 0.82 g, 78%. IR (neat): 2920, 2870, 1682, 1589, 1454, 1438, 1392, 1212, 1160, 1087, 1020, 939, 847, 775, 712, 702, 655, 584, 531 cm^{-1} . ^1H NMR (300 MHz, CDCl_3): δ_{H} = 10.41 (s, 1H), 7.76–6.97 (m, 5H), 5.25 (s, 2H), 4.28 (t, J = 6 Hz, 2H), 3.68 (t, J = 3 Hz, 6H), 2.74 (t, J = 3 Hz, 6H), 1.97–1.88 (m, 2H), 0.37–0.32 (m, 2H). ^{13}C NMR (75 MHz, CDCl_3): δ_{C} = 189.9, 160.8, 142.8, 136.0, 128.5, 122.8, 121.2, 113.2, 62.7, 57.5, 53.4, 50.9, 26.2, 13.0. MS (ES⁺) calcd for $\text{C}_{19}\text{H}_{27}\text{N}_4\text{O}_5\text{Si}$ $[\text{M} + \text{H}]^+$ 419.2, found 419.2; mass fragmentation (EI): 459 (20.7), 458 (26.6), 457 (100), 441 (73.1), 419 (27.4), 297 (21.7), 215 (5.5), 192 (6.8), 174

(24.1), 172 (9.5), 150 (5.0). HRMS (ES⁺) calcd for C₁₉H₂₆N₄O₅Si [M + K]⁺ 457.1309, found 457.1317.

***N*-(1-(3-(Silatranyl)propyl)-1*H*-1,2,3-triazol-4-yl)methylmorpholine (2d).** This compound was synthesized following a similar procedure as for **2a**. However, compound **1d** (1.61 g, 4.32 mmol) and triethanolamine (0.54 g, 3.60 mmol) were used here. M.pt: 124 °C, yield: 1.23 g, 89%. IR (neat): 3336, 3121, 2941, 2879, 1597, 1453, 1324, 1265, 1085, 914, 758, 627, 576 cm⁻¹. ¹H NMR (400 MHz, CDCl₃): δ_H = 7.44 (s, 1H), 4.24 (t, *J* = 7.5 Hz, 2H), 3.70 (t, *J* = 4.2 Hz, 6H), 3.65–3.61 (m, 4H), 3.64 (s, 2H), 2.75 (t, *J* = 4.2 Hz, 6H), 2.54–2.41 (m, 4H), 2.01–1.96 (m, 2H), 0.43–0.39 (m, 2H). ¹³C NMR (100 MHz, CDCl₃): δ_C = 128.3, 121.6, 66.9, 59.4, 57.5, 57.0, 53.4, 51.0, 26.4, 13.2. MS (ES⁺) calcd for C₁₆H₃₀N₅O₄Si [M + H]⁺ 384.2, found 384.2; mass fragmentation (EI): 423 (14.6), 422 (77.7), 385 (20.9), 384 (100), 174 (10.5), 172 (15.5), 150 (8.4), 132 (6.4).

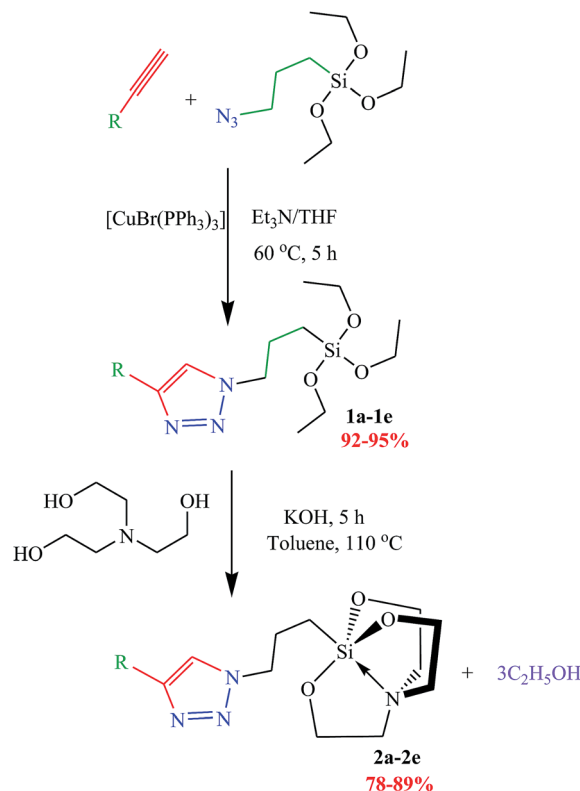
(1-(3-(Silatranyl)propyl)-1*H*-1,2,3-triazol-4-yl)methanol (2e). This compound was synthesized following a similar procedure as for **2a**. However, triethanolamine (0.47 g, 3.18 mmol) and compound **1e** (1.0 g, 3.18 mmol) was used here. M.pt: 143 °C, yield: 1.0 g, 80%, IR (neat): 3364, 3137, 2930, 2875, 1439, 1351, 1271, 1080, 774, 670, 574 cm⁻¹. ¹H NMR (300 MHz, CDCl₃): δ_H = 7.50 (s, 1H), 4.70 (s, 2H), 4.26 (t, *J* = 7.5 Hz, 2H), 3.70 (t, *J* = 5.8 Hz, 6H), 2.75 (t, *J* = 5.8 Hz, 6H), 2.02–1.78 (m, 2H), 1.59 (s, 1H), 0.42–0.23 (m, 2H). ¹³C NMR (75 MHz, CDCl₃): δ_C = 147.4, 121.5, 56.7, 55.3, 52.6, 50.1, 26.0, 13.0. MS (ES⁺) calcd for C₁₂H₂₃N₄O₄Si [M + H]⁺ 315.1, found 315.1; mass fragmentation (EI): 315 (100), 337 (99.2), 338 (14.3), 273 (9.0), 216 (3.1), 192 (14.9), 174 (18.7), 150 (6.4).

Results and discussion

Structural aspects

Scheme 1 illustrates the general synthetic route for the synthesis of TBS-scaffolds (**2a–e**). Initially, azidopropyltriethoxysilane (AzPTES) was prepared by reacting sodium azide with 3-chloropropyltriethoxysilane in dry DMF at 90 °C for 4 h. For the Cu(I)-assisted click silylation of AzPTES, phenyl acetylene, *N*-(prop-2-ynyl)phthalimide, 2-(prop-2-ynyloxy)benzaldehyde, *N*-(propargyl)-morpholine and propargyl alcohol were selected as terminal alkynyl components. The reaction was performed in a very fruitful manner under the [CuBr(PPh₃)₃]-THF/Et₃N system for the synthesis of TBTES-linkers (**1a–e**). The IR spectrum reveals that the characteristic bands of the azido group (–N=N=N, 2091 cm⁻¹) and alkyne groups (–C≡C, 3279 and 2102 cm⁻¹) are no longer present after the click reaction. It is important to discuss here that the ¹H NMR spectra of TBTES-linkers exhibit a triplet around δ ≈ 1.14 ppm and a quartet roughly at δ ≈ 3.65 ppm, corresponding to the CH₃ and OCH₂ of the triethoxysilyl moiety, respectively. The downfield shift of the triplet due to the N₃CH₂ protons from δ = 3.19 to δ ≈ 4.19–4.31 ppm signifies the C–N bond formation resulting in 1,2,3-triazole.

Finally, the transesterification reaction in toluene was successfully carried out between TBTES-linkers (**1a–e**) and triethanolamine in the presence of KOH at 110 °C for 5 h. All TBS-scaffolds (**2a–e**) (Table 2) were isolated as colorless

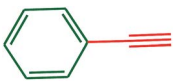
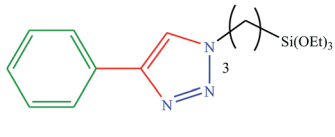
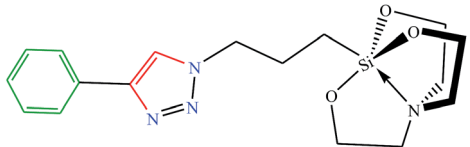
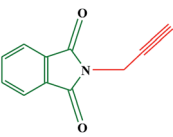
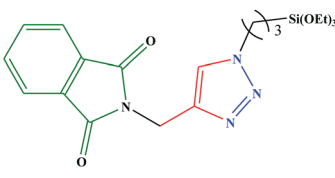
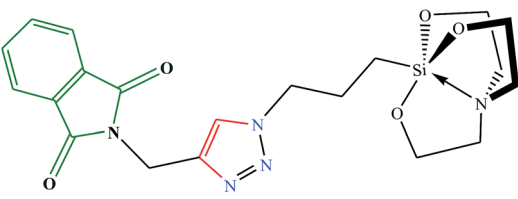
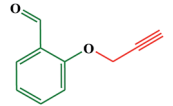
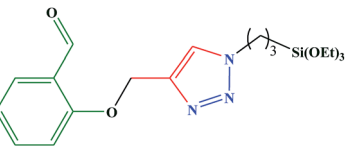
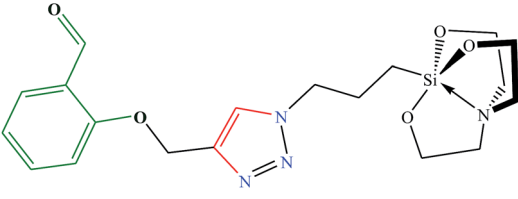
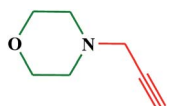
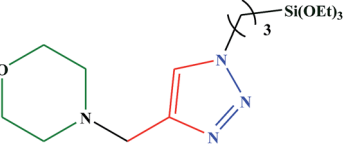
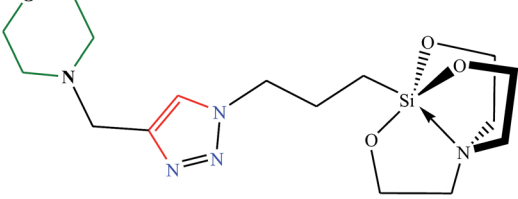

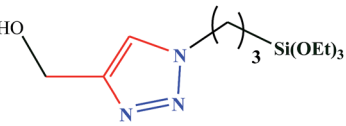
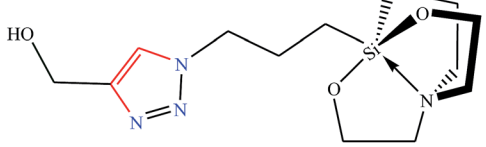


Scheme 1 Synthesis of 1,2,3-triazole-based silatrane (TBS)-scaffolds (**2a–e**).

crystalline solids that are insensitive to air and are characterized by NMR (¹H and ¹³C) and mass spectroscopy. The ¹H NMR spectra of TBS-scaffolds show two intense triplets, a characteristic feature of the Si(OCH₂CH₂)₃N moiety (due to protons of OCH₂, δ ≈ 3.75–3.78 ppm and NCH₂, δ ≈ 2.80–2.83 ppm), which clearly distinguishes silatranes from their parent compounds. In the ¹³C NMR spectra, the methylene carbon of the propyl chain attached to the silicon atom appears as the most shielded carbon atom, which is identified as δ ≈ 12–13 ppm. In the mass spectra of all compounds, the [M + H]⁺ peak appears with a very high intensity along with the [M + Na]⁺ and [M + K]⁺ peaks. Fragmentation patterns of all the TBS-scaffolds follow the general silatrane fragmentation as discussed in literature.⁵²

Crystals of compounds **2a**, **2b**, **2d** and **2e** for the X-ray experiment were grown from the saturated solutions in ethanol–CHCl₃. White, thin, shining, needle-like crystals in star-shaped clusters were isolated at room temperature. The X-ray diffraction study showed that compounds **2a**, **2b**, **2d** and **2e** were crystallized in a monoclinic crystal (Space group *P21/c*), orthorhombic crystal system (Space group = *Pbca*), triclinic crystal system (Space group = *P1*) and monoclinic crystal system (Space group = *C2/c*), respectively. The ORTEP view with atomic labelling (thermal ellipsoids were drawn at 50% probability) of compounds are shown in Fig. 1A–D. X-ray crystal data and structure refinement details are listed in Table 3. Compounds of these types possess a distorted trigonal bipyramidal geometry

Table 2 Synthesized 1,2,3-triazole based silatrane (TBS)-scaffolds (2a–e)

Terminal alkynes ($R-C\equiv C$)		TBTES-linkers (1a–e)		(TBS)-scaffolds (2a–e)	
			Yield (%)		Yield (%)
			92		78
	1a			2a	
			93		89
	1b			2b	
			93		78
	1c			2c	
			95		89
	1d			2d	
			92		80
	1e			2e	

due to the presence of the silatranyl skeleton. The most important parameter in the silatranyl moiety was the Si–N bond length. This Si–N bond was clearly shorter than the sum of the van der Waals radii, which pointed out the weak bonding between both atoms. From the crystal data, it is clear that the effect of the 1,2,3-triazole moiety was not observed on the bond lengths of the silatranyl moiety. This might be due to the presence of a propyl chain between these moieties.

Fluorescence studies

Therefore, by using the click strategy, TBS-scaffolds (2a–e), having binding groups directly attached to the 1,2,3-triazole ring, have been synthesized in good yields, and their affinities towards various biogenic amines were evaluated in a $CH_3CN:H_2O$ (98 : 2; v/v) solvent system. For this assay, eight different biogenic amines were employed and their structures are illustrated in Scheme 2. The interaction of biogenic amines

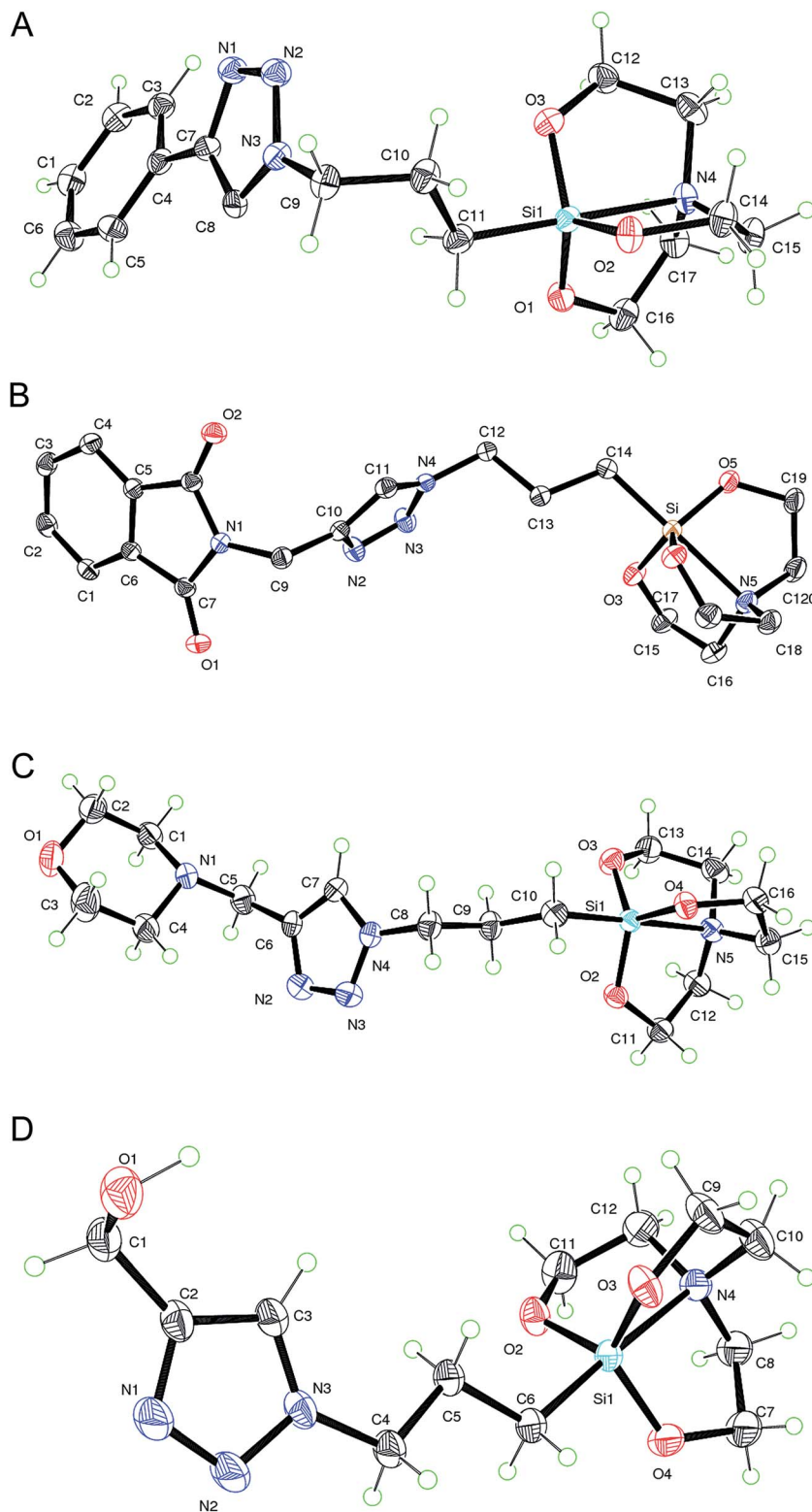


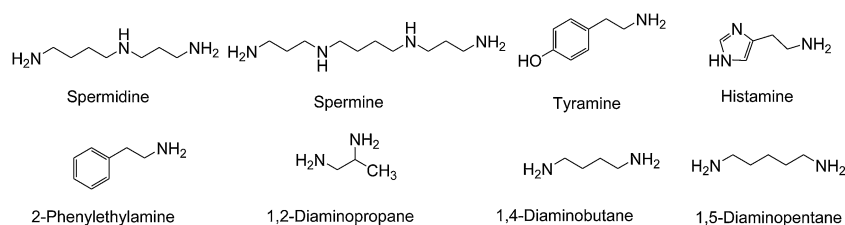
Fig. 1 (A) Showing the ORTEP diagram with numbering scheme for compound **2a** with 50% ellipsoidal probability. (B) Showing the ORTEP diagram with numbering scheme for compound **2b** with 50% ellipsoidal probability. (C) Showing the ORTEP diagram with numbering scheme for compound **2d** with 50% ellipsoidal probability. (D) Showing the ORTEP diagram with numbering scheme for compound **2e** with 50% ellipsoidal probability.

with the TBS-scaffolds (**2a–e**) was evaluated in 5 mL volumetric flasks. As depicted in Fig. S1A,[†] the response of compound **2a** towards biogenic amines remained silent on the fluorescence

spectrophotometer. It did not represent any selectivity towards any particular biogenic amine. Similarly, the effect of biogenic amines on the emission properties of compound **2b** was

Table 3 X-Ray crystal data and structure refinement for compound 2a, 2b, 2d and 2e

Compound	2a	2b	2d	2e
Empirical formula	C ₁₇ H ₂₄ N ₄ O ₃ Si	C ₂₀ H ₂₅ N ₅ O ₅ Si	C ₁₆ H ₂₉ N ₅ O ₄ Si	C ₁₂ H ₂₂ N ₄ O ₄ Si
Formula weight	359.48	443.54	383.53	314.43
Temperature (K)	295(2)	295(2)	295(2)	295(2)
Wavelength (Å)	1.54178	1.54178	1.54178	1.54178
Crystal system	Monoclinic	Orthorhombic	Triclinic	Monoclinic
Space group	<i>P</i> 2 ₁ / <i>c</i>	<i>Pbca</i>	<i>P</i> 1	<i>C</i> 2/ <i>c</i>
Unit cell dimensions				
<i>a</i> (Å)	11.151(5)	22.8796(5)	10.480(5)	23.2106(5)
<i>b</i> (Å)	18.583(5)	7.19450(10)	10.536(5)	11.4407(3)
<i>c</i> (Å)	8.759(5)	25.1019(18)	11.090(5)	14.1836(10)
α /°	90	90	63.047(5)	90
β /°	101.395(5)	90	73.639(5)	127.208(9)
γ /°	90	90	65.682(5)	90
Volume (Å ³)	1779.3(14)	4132.0(3)	987.8(8)	2999.7(2)
<i>Z</i>	4	8	2	8
Calculated density (mg m ^{−3})	1.342	1.426	1.289	1.392
Absorption coefficient (mm ^{−1})	1.375	1.388	1.318	1.592
<i>F</i> (000)	764	1872	412	1344
Crystal size (mm)	0.20 × 0.18 × 0.18	0.20 × 0.18 × 0	0.20 × 0.18 × 0.16	0.20 × 0.18 × 0.18
Theta range for data collection (°)	7.02 to 72.01	6.69 to 72.08	6.86 to 71.96	6.89 to 72.03
Max. and min. transmission	0.7899 and 0.7705	0.8084 and 0.7687	0.8168 and 0.7785	0.7625 and 0.7412
Refinement method	Full-matrix least-squares on <i>F</i> ²	Full-matrix least-squares on <i>F</i> ²	Full-matrix least-squares on <i>F</i> ²	Full-matrix least-squares on <i>F</i> ²
Data/restraints/parameters	3369/0/227	3981/0/280	3631/0/236	2878/0/194
Goodness-of-fit on <i>F</i> ²	1.666	1.150	1.204	1.124
<i>R</i> [<i>I</i> > 2σ(<i>I</i>)]	<i>R</i> ₁ = 0.0519, <i>wR</i> ₂ = 0.1516	<i>R</i> ₁ = 0.0456, <i>wR</i> ₂ = 0.1277	<i>R</i> ₁ = 0.0454, <i>wR</i> ₂ = 0.1276	<i>R</i> ₁ = 0.0530, <i>wR</i> ₂ = 0.1484
<i>R</i> (all data)	<i>R</i> ₁ = 0.0609, <i>wR</i> ₂ = 0.1942	<i>R</i> ₁ = 0.0503, <i>wR</i> ₂ = 0.1295	<i>R</i> ₁ = 0.0534, <i>wR</i> ₂ = 0.1740	<i>R</i> ₁ = 0.0624, <i>wR</i> ₂ = 0.1701
Largest diff. peak and hole (e Å ^{−3})	0.763 and −0.832	0.250 and −0.361	0.527 and −0.676	0.485 and −0.433
CCDC no.	982459	982458	982460	982461



Scheme 2 Biogenic amines used in the present study.

evaluated and represented in Fig. S1B.† The compound **2b** also did not have any significant behavior towards any particular amine. Interestingly, it is observed that **2c** has a high selectivity towards spermine (Fig. 2A). The addition of 70 μM of spermine leads to the enhancement in fluorescence intensity at 393 nm. However, other biogenic amines did not produce any significant change in the emission profile of **2c** except spermine, as shown in Fig. 2B (excitation at 317 nm). The titration was performed to find out the mechanism behind this enhancement. The

titration was accomplished in a 10 mL volumetric flask having a 10 μM solution of **2c** along with the stepwise addition of spermine (Fig. 3A). From the titration, a linear relationship was observed between the fluorescence intensity at 393 nm and the concentration of spermine in the range of 2–50 μM (Fig. 3B). To find out the stoichiometry of complex **2c** spermine, a plot was drawn between [HG] and [H]/([H] + [G]), as shown in Fig. S2A.†⁵³ It has maxima at 0.6, which correspond to 2 : 1 stoichiometry between **2c** and spermine, and has a detection limit of 7 μM. On

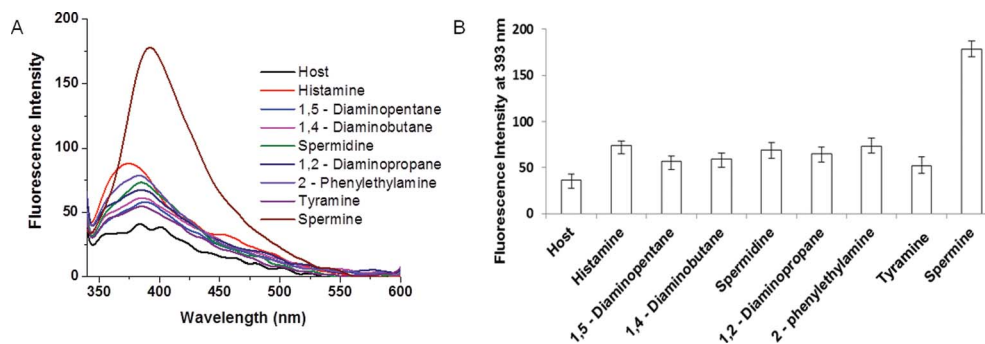


Fig. 2 (A) Fluorescence spectra of **2c** (10 μ M) upon addition of various biogenic amines (histamine, spermine, spermidine, tyramine, 1,2-diaminopropane, 1,4-diaminobutane, 1,5-diaminopentane, 2-phenylethylamine) in $\text{CH}_3\text{CN}-\text{H}_2\text{O}$ (98 : 2; v/v) solvent system (excitation at 317 nm). (B) A change in fluorescence intensity at 393 nm in the presence various biogenic amines (histamine, spermine, spermidine, tyramine, 1,2-diaminopropane, 1,4-diaminobutane, 1,5-diaminopentane, 2-phenylethylamine).

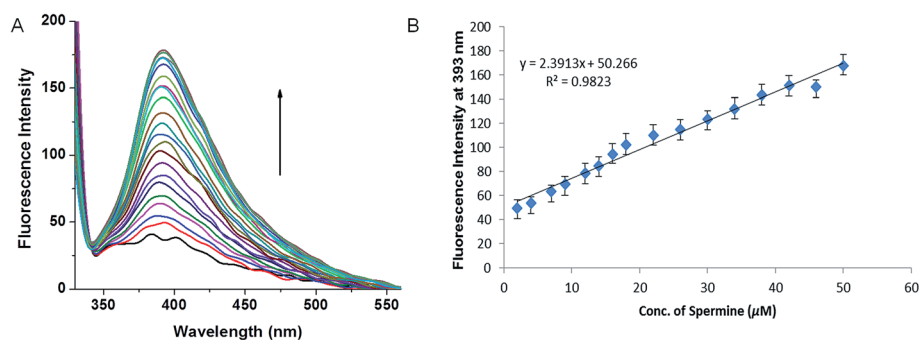
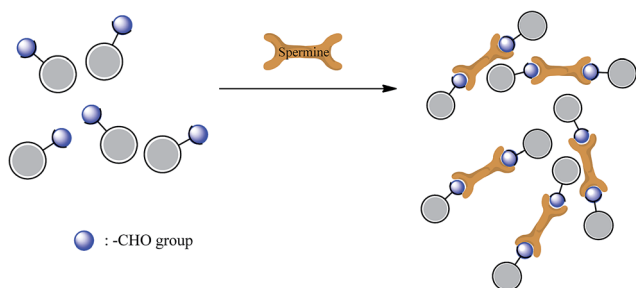


Fig. 3 (A) change in the emission profile of **2c** upon successive addition of spermine in $\text{CH}_3\text{CN}-\text{H}_2\text{O}$ (98 : 2; v/v) solvent system (excitation at 317 nm); (B) The plot between fluorescence intensity at 393 nm and concentration of spermine. The linear relationship was observed in the concentration range of 0 to 50 μ M.

analysis of the titration and Job's plot of **2c**, it was hypothesized that a spermine molecule interact with two molecules of **2c** through a non-covalent interaction, as shown in Scheme 3. These interactions produced a change in the electronic structure of the molecule and cancellation of the PET channel, as a consequence of this enhancement in the intensity of **2c** was observed.⁵⁴ The effect of ionic strength was investigated by using tetrabutyl ammonium perchlorate (0–100 mM). It was observed that with the increase in ionic strength of the solution, the emission profile of **2c** remained the same as shown in Fig. S2B.† Furthermore, to understand the role of medium pH on sensing behavior of **2c**, pH titrations were performed. The

emission profile of **2c** was unchanged in the pH range from 3 to 10 (Fig. S3†).

Inspired by these results and to extend its utility for practical purposes, **2c** was utilized for the sensing of spermine in the urine of a tumor patient. Spermine is found in all eukaryotic cells and is essential for cell growth and proliferation. The increase in the content of spermine in urine may be indicative of a tumor. Therefore, estimation of spermine in the urine of a tumor patient is a good parameter to check the effectiveness of a cancer treatment.^{55–57} Among the various methods of detection, fluorescence spectroscopy is the easiest and simplest technique for the real-time determination of spermine. To perform the assay, two patients who are under the treatment of cholangio carcinoma and carcinoma carcum from last two months are selected, and their urine samples are collected randomly on a day. The urine samples are filtered through Whatman filter paper (4 μ m), followed by centrifugation for 15 min at 400 rpm, and the whole process is repeated thrice. To standardize the procedure, different amounts (10 μ L, 25 μ L, 50 μ L and 100 μ L) of urine samples are added in 10 μ M solution of **2c**. The enhancement in the intensity of **2c** is observed upon addition of urine samples, and the intensity increased linearly with the amount of urine (10 μ L to 100 μ L) except the control sample. In the case of the control sample, enhancement was observed once



Scheme 3 A mechanistic explanation of spermine binding with **2c**.

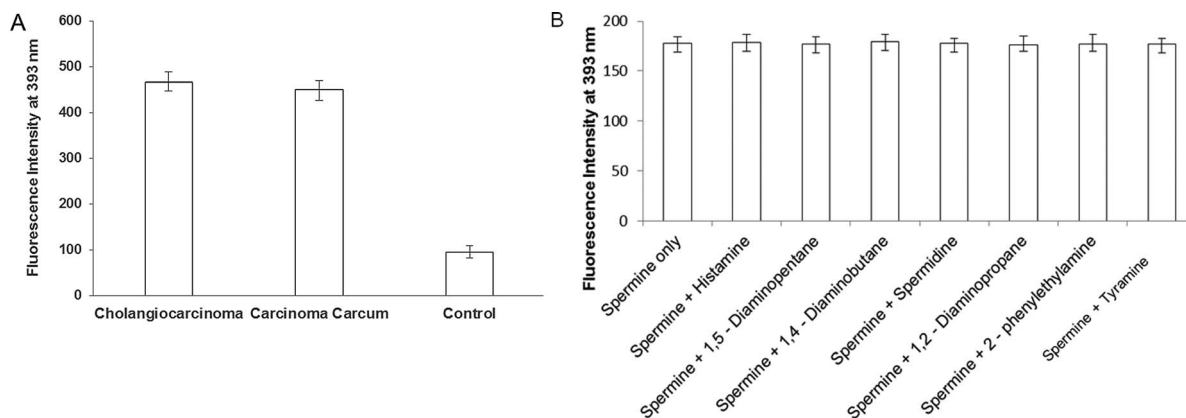


Fig. 4 (A) Fluorescence intensity of receptor **2c** in the urine of cholango carcinoma, carcinoma carcum and healthy person (control) at 393 nm; (B) effect of competing biogenic amines on the selectivity of receptor **2c** towards spermine.

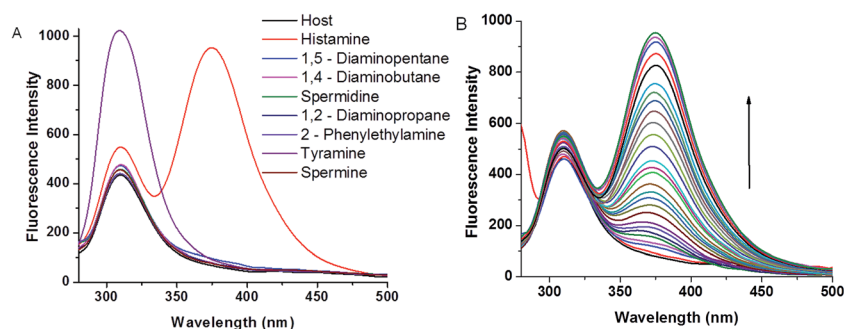


Fig. 5 (A) Fluorescence spectra of **2d** (10 μM) upon addition of various biogenic amines (histamine, spermine, spermidine, tyramine, 1,2-diaminopropane, 1,4-diaminobutane, 1,5-diaminopentane, 2-phenylethylamine) in CH₃CN–H₂O (98 : 2; v/v) solvent system (excitation at 270 nm); (B) change in the emission profile of **2d** upon successive addition of histamine in CH₃CN–H₂O (98 : 2; v/v) solvent system.

upon addition of 10 μL of urine; however, further addition did not cause any change. Therefore, a standardized amount of urine sample (100 μL) was selected for the analysis of spermine. Fig. 4A revealed that addition of 100 μL of urine in 5 mL of **2c** (10 μM) leads to enhancement in fluorescence intensity, which is not so prominent in the control sample. These results increase the scope of this study as well as utility in real

environment. Moreover, it is worth elucidating the effect of other biogenic amines on the selectivity of receptor **2c** towards spermine. Therefore, a set of solutions were prepared, having **2c** (10 μM) along with an equal equivalent of spermine and other competing biogenic amines. As expected, the receptor **2c** has high selectivity even in the presence of other competing biogenic amines (Fig. 4B).

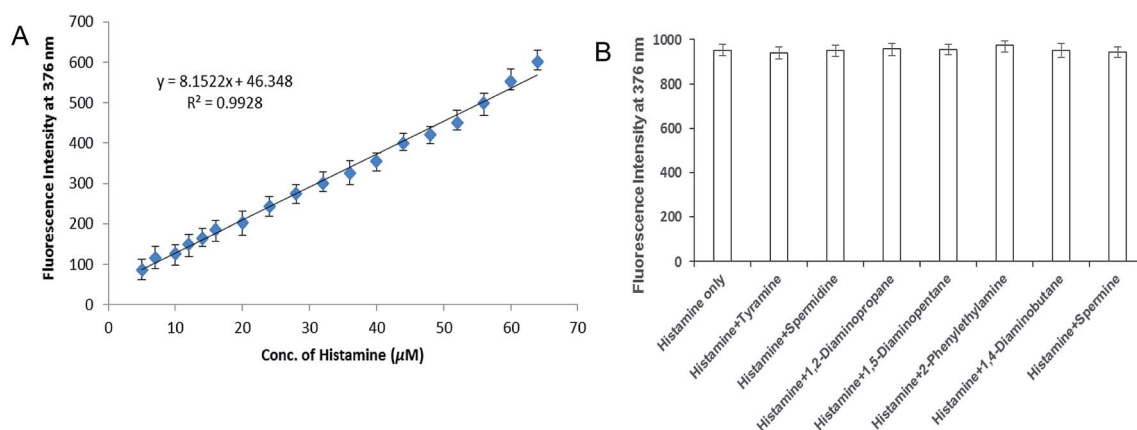


Fig. 6 (A) The plot between fluorescence intensity at 376 nm and concentration of histamine. The linear relationship was observed in the concentration range of 5 to 64 μM; (B) estimation of histamine through **2d** in the presence of other competing bioamines.

In continuation, receptors **2d** and **2e** underwent a biogenic amine assay. Receptor **2d** gave a distinct response towards histamine among other amines; however, receptor **2e** did not show any particular response towards any amine (Fig. S4†). The addition of histamine (100 μM) to the solution of **2d** (10 μM) leads to new band at 376 nm (Fig. 5A). To authenticate the binding, a titration was performed between receptor **2d** and histamine in a 10 mL volumetric flask (Fig. 5B). The successive addition of histamine produced a smooth and linear enhancement in the fluorescence intensity at 376 nm. A calibration plot was drawn between the fluorescence intensity and concentration of histamine and has linearity in the concentration range from 5 to 64 μM , as shown in Fig. 6A. The detection limit has been calculated and it was about 5 μM . The Job's plot was employed to reveal the stoichiometry of the complex **2d** histamine. It has maxima at 0.5, which belongs to a 1 : 1 stoichiometry (Fig. S5†). The possible reason behind the rise of new band upon addition of histamine was ICT. The receptor **2d** has many electronegative groups and these groups form H-bonds with the histamine molecule, which leads to charge transfer within in the molecule and a new band was raised. Furthermore, the selectivity of receptor **2d** towards histamine in the presence of other biogenic amines has been performed. The test was performed in 5 mL volumetric flasks, which contained receptor **2d** along with equal equivalent of histamine and other biogenic amines and placed for 2 h to attain equilibrium. Fig. 6B clearly illustrates the highly selective nature of receptor **2d** towards histamine in the presence other competing amines. The content of histamine has been used as an index for the quality of food. During the storage of food articles different preservatives have been employed. These preservatives have influence on the physiological environment of the cell. Therefore, it is essential to evaluate the effect of ionic strength and pH on the photophysical property of **2d**. It has been observed that ionic strength and pH has a negligible effect on the binding properties of receptor **2d** as shown in Fig. S6† For reproducibility, the relative standard deviation (RSD) of receptor **2c** (2.74%) and receptor **2d** (3.01%) has been calculated ($n = 4$).

Conclusions

We have successfully demonstrated the use of click silylation for the synthesis of fluorogenic organosilicon based chemosensors (TBS-scaffolds) (**2a–e**) from their corresponding TBTES-linkers (**1a–e**). The scope of these TBS-scaffolds was extensively evaluated towards eight different biogenic amines, and the receptors (**2c** and **2d**) proved their high affinity towards spermine and histamine, respectively. The receptor **2c** efficiently detected the increased spermine levels in the urine samples of patients suffering from malignant tumors named Cholangio carcinoma and carcinoma carcum.

Acknowledgements

Authors are thankful to Dr Paramvir Singh Mangat (PGIMER, Chandigarh) for collecting the urine samples of tumors patients.

References

- (a) G. Singh, S. S. Mangat, J. Singh, A. Arora and R. K. Sharma, *Tetrahedron Lett.*, 2014, **55**, 903–909; (b) K. Burglov, N. Moitra, J. Hodacov, X. Cattoen and M. W. C. Man, *J. Org. Chem.*, 2011, **76**, 7326–7333.
- O. D. L. Cobos, B. Fousseret, M. Lejeune, F. Rossignol, M. D. Colas, C. Carrion, C. Boissiere, F. Ribot, C. Sanchez, X. Cattoen, M. W. C. Man and J. O. Durand, *Chem. Mater.*, 2012, **24**, 4337–4342.
- N. Moitra, J. J. E. Moreau, X. Cattoen and M. W. C. Man, *Chem. Commun.*, 2010, **46**, 8416–8418.
- A. Krasinski, V. V. Fokin and K. B. Sharpless, *Org. Lett.*, 2004, **6**, 1237–1240.
- J. Kalisiak, K. B. Sharpless and V. V. Fokin, *Org. Lett.*, 2008, **10**, 3171–3174.
- G. M. Morris, L. G. Green, Z. Radić, P. Taylor, K. B. Sharpless, A. J. Olson and F. Grynszpan, *J. Chem. Inf. Model.*, 2013, **53**, 898–906.
- N. P. Grimster, B. Stump, J. R. Fotsing, T. Weide, T. T. Talley, J. G. Yamauchi, Á. Nemezc, C. Kim, K.-Y. Ho, K. B. Sharpless, P. Taylor and V. V. Fokin, *J. Am. Chem. Soc.*, 2012, **134**, 6732–6740.
- S. W. Millward, R. K. Henning, G. A. Kwong, S. Pitram, H. D. Agnew, K. M. Deyle, A. Nag, J. Hein, S. S. Lee, J. Lim, J. A. Pfeilsticker, K. B. Sharpless and J. R. Heath, *J. Am. Chem. Soc.*, 2011, **133**, 18280–18288.
- T. Weide, S. A. Saldanha, D. Minond, T. P. Spicer, J. R. Fotsing, M. Spaargaren, J. M. Frère, C. Bebrone, K. B. Sharpless, P. S. Hodder and V. V. Fokin, *ACS Med. Chem. Lett.*, 2010, **1**, 150–154.
- C. A. Valdez, J. C. Tripp, Y. Miyamoto, J. Kalisiak, P. Hruz, Y. S. Andersen, S. E. Brown, K. Kangas, L. V. Arzu, B. J. Davids, F. D. Gillin, J. A. Upcroft, P. Upcroft, V. V. Fokin, D. K. Smith, K. B. Sharpless and L. Eckmann, *J. Med. Chem.*, 2009, **52**, 4038–4053.
- D. K. Dalvie, A. S. Kalgutkar, S. C. Khojasteh-Bakht, R. S. Obach and J. P. O'Donnell, *Chem. Res. Toxicol.*, 2002, **15**, 269–299.
- J. K. Puri, R. Singh and V. K. Chahal, *Chem. Soc. Rev.*, 2011, **40**, 1791–1840.
- (a) R. R. Holmes, *Chem. Rev.*, 1990, **90**, 17–31; (b) R. R. Holmes, *Chem. Rev.*, 1996, **96**, 927–950; (c) R. J. P. Corriu, *J. Organomet. Chem.*, 1990, **400**, 81–106; (d) C. Chuit, R. J. P. Corriu, C. Reye and J. C. Young, *Chem. Rev.*, 1993, **93**, 1371–1448.
- (a) B. J. Brennan, A. E. Keirstead, P. A. Liddell, S. A. Vail, T. A. Moore, A. L. Moore and D. Gust, *Nanotechnology*, 2009, **20**, 505203; (b) C. L. Frye, G. E. Vogel and J. A. Hall, *J. Am. Chem. Soc.*, 1961, **83**, 996–997.
- R. Singh, J. K. Puri, R. P. Sharma, A. K. Malik and V. Ferretti, *J. Mol. Struct.*, 2010, **982**, 107–112.
- A. Kaur, H. Sharma, S. Kaur, N. Singh and N. Kaur, *RSC Adv.*, 2013, **3**, 6160–6166.
- U. Fegade, H. Sharma, S. Attarde, N. Singh and A. Kuwar, *J. Fluoresc.*, 2013, 1–11.

- 18 H. Sharma, A. Singh, N. Kaur and N. Singh, *ACS Sustainable Chem. Eng.*, 2013, **1**, 1600–1608.
- 19 H. Sharma, V. K. Bhardwaj, N. Kaur, N. Singh and D. O. Jang, *Tetrahedron Lett.*, 2013, **54**, 5967–5970.
- 20 M. J. Kim, H. Sharma, N. Singh and D. O. Jang, *Inorg. Chem. Commun.*, 2013, **36**, 96–99.
- 21 H. Sharma, H. J. Guadalupe, J. Narayanan, H. Hofeld, T. Pandiyan and N. Singh, *Anal. Methods*, 2013, **5**, 3880–3887.
- 22 C. W. Tabor and H. Tabor, *Annu. Rev. Biochem.*, 1984, **53**, 749–790.
- 23 B. G. Cipolla, J. Ziade, J. Y. Bansard, J. P. Moulinoux, F. Staerman, V. Quemener, B. Lobel and F. Guille, *Cancer*, 1996, **78**, 1055–1065.
- 24 P. Celano, S. B. Baylin and R. A. Casero, *J. Biol. Chem.*, 1989, **264**, 8922–8927.
- 25 B. G. Feuerstein, N. Pattabiraman and L. J. Marton, *Nucleic Acids Res.*, 1990, **18**, 1271–1282.
- 26 B. Brune, P. Hartzell, P. Nicotera and S. Orrenius, *Exp. Cell Res.*, 1991, **195**, 323–329.
- 27 A. U. Khan, Y. H. Mei and T. Wilson, *Proc. Natl. Acad. Sci. U. S. A.*, 1992, **89**, 11426–11427.
- 28 U. Khan, P. D. Mascio, M. H. G. Medeiros and T. Wilson, *Proc. Natl. Acad. Sci. U. S. A.*, 1992, **89**, 11428–11430.
- 29 X. Yang and G. A. Rechnitz, *Electroanalysis*, 1995, **7**, 105–108.
- 30 Z. Kostereli and K. Severin, *Chem. Commun.*, 2012, **48**, 5841–5843.
- 31 W. F. Staruszkiewicz and J. F. Bond, *J.-Assoc. Off. Anal. Chem.*, 1981, **64**, 584–591.
- 32 P. Nadeau, S. Delaney and L. Chouinard, *Plant Physiol.*, 1987, **84**, 73–77.
- 33 A. R. G. Dibble, P. J. Davies and M. A. Mutscler, *Plant Physiol.*, 1988, **86**, 338–340.
- 34 R. Reggiani, P. Giussani and A. Bertani, *Plant Cell Physiol.*, 1990, **31**, 489–494.
- 35 P. G. Zambonin, A. Guerrieri, T. Rotunno and F. Palmisano, *Anal. Chim. Acta*, 1991, **251**, 101–107.
- 36 P. J. Oefner, S. Wongyai and G. Bonn, *Clin. Chim. Acta*, 1992, **205**, 11–18.
- 37 M. Z. Hauschild, *J. Chromatogr.*, 1993, **630**, 397–401.
- 38 T. Hyvonen, T. A. Keinänen, A. R. Khomutov and T. O. Eloranta, *J. Chromatogr.*, 1992, **574**, 17–21.
- 39 H. Ohta, Y. Takeda, K. I. Yoza and Y. Nogata, *J. Chromatogr.*, 1993, **628**, 199–215.
- 40 D. Tanima, Y. Imamura, T. Kawabata and K. Tsubaki, *Org. Biomol. Chem.*, 2009, **7**, 4689–4694.
- 41 N. Kielland, M. Vendrell, R. Lavilla and Y.-T. Chang, *Chem. Commun.*, 2012, **48**, 7401–7403.
- 42 Y. Yano, K. Yokoyama, E. Tamiya and I. Karube, *Anal. Chim. Acta*, 1996, **320**, 269–276.
- 43 T. I. Kim, J. Park and Y. Kim, *Chem.-Eur. J.*, 2011, **17**, 11978–11982.
- 44 M. Ikeda, T. Yoshii, T. Matsui, T. Tanida, H. Komatsu and I. Hamachi, *J. Am. Chem. Soc.*, 2011, **133**, 1670–1673.
- 45 B. Lee, R. Scopelliti and K. Severin, *Chem. Commun.*, 2011, **47**, 9639–9641.
- 46 K. J. Cash and H. A. Clark, *Anal. Chem.*, 2013, **85**, 6312–6318.
- 47 J. Lange and C. Wittmann, *Anal. Bioanal. Chem.*, 2002, **372**, 276–283.
- 48 J. Plonka, *Anal. Methods*, 2012, **4**, 3071–3094.
- 49 A. I. Vogel, *A Text Book of Practical Organic Chemistry*, Longman, London, 4th edn, 1978.
- 50 P. Job, *Ann. Chim.*, 1928, **9**, 113–203.
- 51 (a) Rigaku, *CrystalClear, Version 1.4.0*, Rigaku Americas Corporation, The Woodlands, Texas, USA, 2005; (b) Rigaku, *PROCESS-AUTO*, Rigaku Corporation, Tokyo, Japan, 1998; (c) G. M. Sheldrick, *Acta Crystallogr., Sect. A: Found. Crystallogr.*, 2008, **64**, 112–122; (d) A. Altomare, M. C. Burla, M. Camalli, G. L. Cascarano, C. Giacovazzo, A. Guagliardi, A. G. G. Moliterni, G. Polidori and R. Spagna, *J. Appl. Crystallogr.*, 1999, **32**, 115–119; (e) G. M. Sheldrick, *SHELXS-97. Program for the Solution of Crystal Structures*, University of Göttingen, Germany, 1997; (f) L. J. Farrugia, *J. Appl. Crystallogr.*, 1999, **32**, 837–838.
- 52 J. K. Puri, R. Singh, V. K. Chahal, R. P. Sharma, J. Wagler and E. Kroke, *J. Organomet. Chem.*, 2011, **696**, 1341–1348.
- 53 M. Nakamura, T. Sanji and M. Tanaka, *Chem.-Eur. J.*, 2011, **17**, 5344–5349.
- 54 C. Moinard, L. Cynober and J. P. Bant, *Clin. Nutr.*, 2005, **24**, 184–197.
- 55 D. H. Russel, *Clin. Chem.*, 1977, **23**, 22–27.
- 56 T. M. Wager, *J. Am. Chem. Soc.*, 2007, **129**, 16020–16028.
- 57 D. H. Russel, *Nature*, 1971, **233**, 144–145.